Precision calculation of isospin-symmetry-breaking corrections to $T = 1/2$ mirror decays using configuration-interaction framework built upon multireference charge-dependent density functional theory

M. Konieczka◉, P. Bączyk◉, and W. Satuła◉

Institute of Theoretical Physics, Faculty of Physics, University of Warsaw, ul. Pasteura 5, PL-02-093 Warsaw, Poland

Background: Theoretical approaches based on energy density functionals (EDF) are gaining in popularity due to their broad range of applicability. One of their key features is the proper treatment of symmetries of the nuclear interaction. It is because of this that EDF-based methods may provide another independent verification of foundations of the standard model, i.e., the assumption that hadronic structure of matter is indeed built upon three generations of quarks. However, such a study cannot be precisely performed without including very subtle isospin-symmetry-breaking (ISB) terms both in the long- and short-range part of the nuclear interaction. Only very recently, the latter part of ISB interaction has been successfully adapted to EDF to describe Nolen-Shiffer anomaly.

Purpose: The aim of the paper is to study the impact of the short-range ISB terms on isospin impurities in the wave functions of $T = 1/2$ mirrors (α_{ISB}) and the ISB corrections to their Fermi decays (δ_{ISB}). The consequent purpose is to eventually lead the calculation towards evaluation of the V_{ud} matrix element of Cabbibo-Kobayashy-Maskawa (CKM) quark mixing matrix.

Methods: We use multireference density functional theory (MR-DFT) that conserves angular-momentum and properly treats isospin. Moreover, for the very first time, the functional includes both short- and long-range isospin-symmetry-breaking forces. Calculations are performed using three different variants of the ISB interaction: (i) involving only the Coulomb force, (ii) involving the Coulomb and leading-order (LO) contact isovector forces, and (iii) involving the Coulomb and next-to-leading-order (NLO) contact isovector forces. The evaluation of V_{ud} matrix element requires more subtle approach involving configuration mixing. For this reason, the calculation is performed with DFT-rooted no core configuration interaction (DFT-NCCI) model including above-mentioned ISB terms as well.

Results: We compute isospin impurities and ISB corrections in $T = 1/2$ mirrors ranging from $A = 11$–47 with MR-DFT formalism. Next, we focus on the best measured $A = 19, 21, 35$, and 37 mirror pairs, calculate the ISB corrections to their Fermi decays with DFT-rooted NCCI method and then extract V_{ud} matrix element. The final result shows that $V_{\text{ud}} = 0.9736(16)$, which (central value) is in a good agreement with the value assessed from the superallowed $0^+ \rightarrow 0^+$ Fermi transitions and is only slightly above the value obtained using state-of-the-art shell model. Last but not least, we demonstrate the stability of our calculation.

Conclusions: The isovector short-range interaction surprisingly strongly influences the isospin impurities and ISB corrections in the $T = 1/2$ mirrors as compared to the calculation where Coulomb interaction is the only source of the isospin-symmetry-breaking. Moreover, V_{ud} matrix element is sensitive to the short-range isovector terms in the interaction and can be successfully extracted within DFT-rooted approach that includes configuration mixing.

I. INTRODUCTION

With high-precision experiments and theoretical modeling of atomic nuclei one can test fundamental equations governing properties of subatomic matter. Of particular interest are processes used to search for possible signals of new physics beyond the standard model (SM) such as the superallowed $0^+ \rightarrow 0^+$ β decays, see Refs. [1,2] and references quoted therein. With small, of order of a percent, theoretical corrections accounting for radiative processes and isospin-symmetry breaking (ISB), these pure Fermi (vector) decays allow us to verify the conserved vector current (CVC) hypothesis with a very high precision. In turn, they provide the most precise values of the leading element, V_{ud}, of the Cabbibo-Kobayashi-Maskawa (CKM) matrix.

The mixed Fermi-Gamow-Teller decays of $T = 1/2$ mirror nuclei, which are a subject of this work, offer an alternative way for the SM tests [3,4] provided that another observable such as the β-neutrino correlation (a), β-asymmetry (A), or neutrino-asymmetry (B) coefficient is measured with high accuracy. The SM expressions for a_{SM}, A_{SM}, and B_{SM} can be found, for example, in the review [5]. These coefficients

depend on angular momenta of the participating nuclear states and a mixing ratio ϱ of the Gamow-Teller (M_{GT}) and Fermi (M_F) matrix elements:

$$\varrho = \frac{g_A M_{GT}}{g_V M_F}, \tag{1}$$

where $g_{V/A}$ are vector and axial-vector electroweak currents coupling constants, respectively. Precision measurements of a_{SM}, A_{SM}, or B_{SM} provide, therefore, empirical values of ϱ, which are instrumental for the V_{ud} calculation since they allow us to avoid using theoretical values of ϱ which, in spite of a recent progress in the *ab initio* GT-decay calculation [6], are not yet accurate enough to be directly used for that purpose. With the experimental ϱ the V_{ud} calculation depends upon precision measurement of the partial lifetime and theoretically calculated radiative (δ'_R, δ^V_{NS}, Δ^V_R) and many-body ISB (δ^V_{ISB}) corrections to the Fermi branch. The latter are defined together with δ^V_{NS} as a deviation from Fermi matrix element in its isospin-symmetry limit M^0_F:

$$|M_F|^2 = |M^0_F|^2 (1 + \delta^V_{NS} - \delta^V_{ISB}). \tag{2}$$

Indeed, the reduced lifetime for an allowed semileptonic β decay of $T = 1/2$ mirror nuclei can be written as [3,4]:

$$\begin{aligned}\mathcal{F}t^{mirror} &\equiv f_V t (1 + \delta'_R)(1 + \delta^V_{NS} - \delta^V_{ISB}) \\ &= \frac{K}{G^2_F V^2_{ud} C^2_V (1 + \Delta^V_R)\left(1 + \frac{f_A}{f_V}\varrho^2\right)}, \end{aligned} \tag{3}$$

where $K/(\hbar c)^6 = 2\pi^3 \hbar \ln 2/(m_e c^2)^5 = 8120.2787(11) \times 10^{-10}$ GeV^{-4}s is a universal constant, G_F is the Fermi-decay coupling constant equal $G_F/(\hbar c)^3 = 1.16637(1) \times 10^{-5}$ GeV^{-2}, and $f_{V/A}$ denote phase space factors. Hence, similar to the superallowed $0^+ \rightarrow 0^+$ decays, the quality of the test depends on the accuracy of empirical data and the quality of theoretical models used to compute the corrections, in particular the many-body δ^V_{ISB} corrections, which are a subject of this work. Current precision of $T = 1/2$ mirror decay experiments is achieved only for a handful of isotopes, which is still not enough for stringent testing of the SM. Fast progress in β-decay correlation techniques though opens up new opportunities and keeps the field vibrant see, for example, Ref. [7] for the recent high-precision β-asymmetry measurement in ^{37}K decay.

The goal of this work is to study the impact of isovector effective contact interaction that is adjusted to account for the Nolen-Schiffer anomaly [8] in nuclear masses on isospin impurities in the wave functions of $T = 1/2$ mirrors, the isospin symmetry-breaking (ISB) corrections to their Fermi decays, and the V_{ud} matrix element in sd-shell $T = 1/2$ mirror nuclei. We use different variants of symmetry-restored density functional theory (DFT), which were successfully applied in the past to compute isospin impurities and ISB corrections to superallowed $0^+ \rightarrow 0^+$ decays, see Refs. [9,10]. After brief presentation of the methods in Sec. II we demonstrate that the class-III local force strongly affects the calculated isospin impurities, see Sec. III A. This rather counterintuitive observation sparked a motivation for undertaking a detailed theoretical study of the ISB corrections to the Fermi branch of $T = 1/2$ ground-state decays. In this context, in the first place,

we present isospin and angular-momentum projected multireference DFT calculations covering $T = 1/2$ nuclei with $11 \leqslant A \leqslant 47$, see Sec. III A. Next, in Sec. III B, we focus on decays of $A = 19$, 21, 35, and 37 mirror nuclei for which experimental data on correlation parameters are precise enough to allow for extracting V_{ud} matrix element. For these cases we perform the DFT-based no-core-configuration-interaction calculations (DFT-NCCI), see Ref. [11] for details, including theoretical uncertainty analysis, see Sec. III C. The paper is summarized in Sec. IV.

II. METHODS

The nuclear mean-field-based models are almost perfectly tailored to study the ISB effects. The single-reference DFT (SR-DFT) treats Coulomb polarization properly, without involving an approximation of an inert core, and accounts for an interplay between short- and long-range forces in a self-consistent way. The spontaneous symmetry breaking (SSB) effects that accompany the SR-DFT solutions and introduce, in particular, spurious isospin impurities and angular-momentum nonconservation can be then taken care of by extending the framework beyond mean field to multireference level (MR-DFT) with an aid of isospin- and angular-momentum projection techniques [9,10,12]. However, the nuclear energy density functionals (EDF), which are conventionally applied in the DFT-based calculations use Coulomb as the only source of ISB. Therefore they are incomplete in the context of the ISB studies and cannot fully describe ISB observables such as triplet (TDE) or mirror displacement energies (MDE) of nuclear binding energies. The latter deficiency is known in the literature under the name of Nolen-Schiffer anomaly [8]. There is a consensus that these deficiencies cannot be cured without introducing non-Coulombic sources of ISB as shown within the nuclear shell model (NSM), Hartree-Fock (HF) theory or *ab initio* calculations in Refs. [13–20] and references given therein.

Recently, we constructed the single-reference charge-dependent DFT (SR-CDDFT) that includes, apart of the Coulomb and isoscalar Skyrme interactions, the leading-order (LO) [21] zero-range and next-to-leading order (NLO) [22] gradient interactions of class II, which introduces charge-independence breaking (CIB) and class III describing charge-symmetry-breaking (CSB) effects in the Henley and Miller classification [23,24]. We have subsequently demonstrated that the SR-CDDFT allows for very accurate treatment of MDEs and TDEs in a very broad range of masses already in LO [21] and showed that the description can be further improved by adding NLO terms [22]. In Ref. [22] we have also provided the arguments that the newly introduced ISB terms model strong-force-related effects of CIB and CSB rather than the beyond-mean-field electromagnetic corrections.

The aim of this work is to extend the SR-CDDFT to MR-CDDFT and perform a systematic study of the isospin impurities and ISB corrections to the beta decays in $T = 1/2$ mirrors. In this case the ISB effects due to class II or class IV forces are negligible [17,21,22]. Therefore, non-Coulombic ISB force can be approximated by the isovector effective

interaction up to NLO in the effective theory expansion:

$$\hat{V}^{\mathrm{III}}(i, j) = \left(t_0^{\mathrm{III}}\, \delta(\boldsymbol{r}_{ij}) + \tfrac{1}{2} t_1^{\mathrm{III}}[\delta(\boldsymbol{r}_{ij})\boldsymbol{k}^2 + \boldsymbol{k}'^2 \delta(\boldsymbol{r}_{ij})] \right.$$
$$\left. + t_2^{\mathrm{III}}\boldsymbol{k}' \delta(\boldsymbol{r}_{ij})\boldsymbol{k} \right) \left(\hat{\tau}_3^{(i)} + \hat{\tau}_3^{(j)} \right), \qquad (4)$$

where $\boldsymbol{k} = \frac{1}{2i}(\boldsymbol{\nabla}_i - \boldsymbol{\nabla}_j)\, [\boldsymbol{k}' = -\frac{1}{2i}(\boldsymbol{\nabla}_i - \boldsymbol{\nabla}_j)]$ are relative momentum operators acting to the right (left), respectively.

The essence of MR-DFT is to cure the spurious effects of SSB. The procedure boils down to a rediagonalization of the entire Hamiltonian in a good isospin and good angular-momentum basis generated by acting on HF configuration $|\varphi\rangle$ with the standard one-dimensional (1D) isospin $\hat{P}_{T_z T_z}^T$ and 3D angular-momentum $\hat{P}_{MK}^I$ projection operators:

$$|\varphi;\, IMK;\, TT_z\rangle = \frac{1}{\sqrt{N_{\varphi;IMK;TT_z}}} \hat{P}_{T_z T_z}^T \hat{P}_{MK}^I |\varphi\rangle, \qquad (5)$$

where

$$\hat{P}_{T_z,T_z}^T = \frac{2T+1}{2} \int_0^\pi d_{T_z T_z}^T(\beta_T) \hat{R}(\beta_T) \sin\beta_T\, d\beta_T, \qquad (6)$$

$$\hat{P}_{M,K}^I = \frac{2I+1}{8\pi^2} \int D_{MK}^{I*}(\Omega) \hat{R}(\Omega)\, d\Omega. \qquad (7)$$

Here, $\hat{R}(\beta_T) = e^{-i\beta_T \hat{T}_y}$ stands for the rotation operator about the y axis in the isospace, $d_{T_z T_z}^T(\beta_T)$ is the Wigner function, and $T_z = (N-Z)/2$ is the third component of the total isospin $\boldsymbol{T}$ while $\hat{R}(\Omega) = e^{-i\gamma\hat{J}_z} e^{-i\beta\hat{J}_y} e^{-i\alpha\hat{J}_z}$ is the three-dimensional rotation operator in space, $\Omega = (\alpha, \beta, \gamma)$ are the Euler angles, $D_{MK}^I(\Omega)$ is the Wigner function, and M and K denote the angular-momentum components along the laboratory and intrinsic z axis, respectively [25,26].

Due to overcompleteness of the set (5), the rediagonalization of the Hamiltonian is performed by solving the Hill-Wheeler-Griffin equation in the collective space — a subspace spanned by the linearly independent natural states $|\varphi;\, IM;\, TT_z\rangle^{(i)}$ accounting for the K mixing, see Ref. [27], for further details. The resulting eigenfunctions are

$$|n;\, \varphi;\, IM;\, T_z\rangle = \sum_{i,T \geqslant |T_z|} b_{iT}^{(nI;\varphi)} |\varphi;\, IM;\, TT_z\rangle^{(i)}, \qquad (8)$$

where n enumerates eigenstates in ascending order according to their energies. The quantum state (8) is free from spurious isospin mixing.

Let us observe that, contrary to SR-DFT, which uses one Slater determinant (single reference state) and is therefore a true mean-field theory, MR-DFT goes evidently beyond mean-field approximation. Indeed, the state (5) is a linear (continuous) combination of Slater determinants rotated in space and isospace $|\varphi(\Omega, \beta_{\mathrm{T}})\rangle \equiv \hat{R}(\Omega)\hat{R}(\beta_{\mathrm{T}})|\varphi\rangle$ weighted with appropriate (symmetry dictated) Wigner D functions, which cannot be cast into a single Slater determinant. Since the MR-DFT uses only one mean-field state $|\varphi\rangle$ representing concrete self-consistent nucleonic configuration the expansion coefficients in good angular momentum and isospin basis (5) can be interpreted as mean-field isospin impurities. It is well known, however, that these numbers contain substantial amount of unphysical isospin mixing [9] and, as such, cannot be compared to experiment. In order to remove unphysical

mixing one has to rediagonalize the Hamiltonian in good isospin basis. Moreover, since the MR-DFT uses one configuration the wave function may not be equipped with the correlation coming from higher excitations or, as it will be demonstrated below, can inherit certain bad features of the underlying mean-field configuration. These deficiencies can be compensated by applying configuration mixing in DFT-NCCI formalism.

The DFT-NCCI scheme proceeds as follows. One starts with computation of relevant (multi)particle-(multi)hole deformed HF configurations φ_i. Next, with an aid of projection methods, one computes a set of projected states $|\varphi_i;\, IMK;\, TT_z\rangle$, see Eq. (5), which are subsequently mixed to account for K mixing and physical isospin mixing. At this stage one obtains a set of nonorthogonal states $|n;\, \varphi_i;\, IM;\, T_z\rangle$ of Eq. (8), which are eventually mixed by solving the Hill-Wheeler-Griffin equation. In the mixing we use the same Hamiltonian that was used to create the HF configurations. Further details concerning the DFT-NCCI scheme can be found in Ref. [11].

All calculations presented below were done using the code HFODD [28] with the SV$_{\mathrm{SO}}$ Skyrme force, a variant of the SV EDF of Ref. [29] with the tensor terms included and the spin-orbit strength increased by a factor of 1.2 as proposed in Ref. [30]. The code includes the local ISB EDF, in the LO and NLO variants, and allows for simultaneous 1D isospin and 3D angular-momentum projections, and is also equipped with the DFT-NCCI module. In the following we compare three variants of the calculations including different ISB forces: (i) involving only the Coulomb force ($\hat{V}_{\mathrm{C}}$), (ii) involving the Coulomb and LO contact ISB forces ($\hat{V}_{\mathrm{C}} + \hat{V}_{\mathrm{LO}}^{\mathrm{III}}$), and (iii) involving the Coulomb and NLO local ISB forces ($\hat{V}_{\mathrm{C}} + \hat{V}_{\mathrm{NLO}}^{\mathrm{III}}$). These variants will be labeled by the acronyms C, LO, and NLO, respectively.

III. RESULTS

A. Influence of zero-range isovector interaction on isospin impurities and ISB corrections to Fermi β decays

Contribution to MDE in $T = 1/2$ mirror nuclei due to the contact class-III interaction constitutes, on average, around 7–8 % of the contribution coming from the Coulomb force as shown in Refs. [21,22]. One would therefore naively expect that the class-III ISB force would also have a rather modest impact on the isospin impurity in the nth state of spin I: $\alpha_{\mathrm{ISB}}^{(n)} = 1 - \sum_i |b_{iT=|T_z|}^{(nI;\varphi)}|^2$. Figure 1 shows arithmetic means

$$\bar{\alpha}_{\mathrm{ISB}}(A) = [\alpha_{\mathrm{ISB}}(A, T_z = 1/2) + \alpha_{\mathrm{ISB}}(A, T_z = -1/2)]/2$$

in the ground states of $T_z = \pm 1/2$ for $11 \leqslant A \leqslant 47$. The curves illustrate impurities obtained using C (α_{C}), LO (α_{LO}), and NLO (α_{NLO}) variants of the ISB interaction with parameters taken from Ref. [22].

It is surprising to see that the local class-III force strongly increases isospin mixing. The relative difference between α_{LO} and α_{C} gradually decreases with A (see insert in Fig. 1) from 90% to approximately 40% (50%) in the lower fp-shell nuclei for the LO (NLO) theory, respectively. Note also that the NLO theory brings much smaller increase of α_{ISB} as compared to
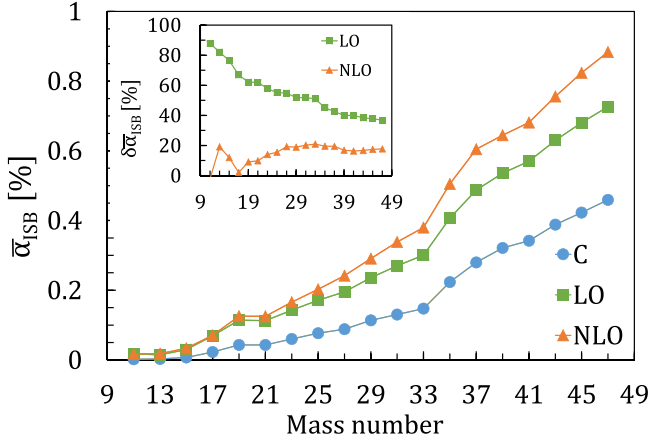
FIG. 1. Arithmetic means of $\bar\alpha_C$ (blue), $\bar\alpha_{LO}$ (green), and $\bar\alpha_{NLO}$ (orange) over the ground-state values in $T_z = \pm 1/2$ mirror partners versus A. The insert shows relative differences $\delta\bar\alpha_{LO} \equiv \frac{\bar\alpha_{LO} - \bar\alpha_C}{\bar\alpha_{LO}}$ and $\delta\bar\alpha_{NLO} \equiv \frac{\bar\alpha_{NLO} - \bar\alpha_{LO}}{\bar\alpha_{NLO}}$.

FIG. 2. ISB corrections to the Fermi branch of ground-state β decay in $T = 1/2$ mirror nuclei calculated using variants C (blue dots), LO (green squares), and NLO (orange triangles) of our MR-DFT model.

the LO what is expected for a converging effective theory. We have also verified (using isospin-projected theory) that strong increase in α_{ISB} due to class-III force takes place for density-dependent popular Skyrme forces such as SLy4 [31].

The additional isospin mixing introduced by ISB contact terms, see Eq. (4), is expected to impact the ISB corrections to the Fermi branch in mirror β decays. In order to assess the effect quantitatively we performed systematic calculation of δ^V_{ISB} in $11 \leqslant A \leqslant 47$ using the SV$_{SO}$ Skyrme force and three variants C, LO, and NLO of the ISB forces. Since the precision is of utmost importance we refitted the class-III ISB interaction and adjusted its parameters to MDEs in $11 \leqslant A \leqslant 47$ calculated at the MR-DFT level. The fit gives $t^{III}_0 = -6.3 \pm 0.3$ MeV fm^3 for the SV$^{LO}_{SO}$ functional and $t^{III}_0 = 0 \pm 2$ MeV fm^3, $t^{III}_1 = -2 \pm 2$ MeV fm^5, and $t^{III}_2 = -4 \pm 1$ MeV fm^5 for the SV$^{NLO}_{SO}$ functional. In the latter case we observed that the t^{III}_0 and t^{III}_1 parameters are strongly correlated, which increases their theoretical uncertainty and, in turn, the uncertainty on the calculated δ^V_{ISB}. The results of δ^V_{ISB} calculation are presented in Fig. 2. As anticipated, an enhancement in α_{ISB} implies strong enhancement in δ^V_{ISB}, of the order of 70% on average, caused by the LO term and further, albeit as expected much smaller, increase obtained in the NLO calculation.

B. Evaluation of V_{ud} matrix element in DFT-NCCI calculation

The calculated δ^V_{ISB} versus A curve shows two irregularities for $A = 19$ and $A = 37$. Such irregularities indicate enhanced mixing among single-particle Nilsson orbitals and, indirectly, suggest that the MR-DFT calculations are not sufficient. Similar problems were encountered already in our seminal MR-DFT calculation of δ^V_C for $0^+ \to 0^+$ superallowed Fermi decays in $A = 38$ (and $A = 18$) cases, see Ref. [10]. The value of δ^V_C calculated in Ref. [10] for $A = 38$ was anomalously large due to accidental near degeneracy and very strong mixing of the Nilsson orbitals originating from the $1s_{1/2}$ and $0d_{3/2}$ spherical subshells. Within the MR-DFT framework (involving projection from a single Slater determinant) such
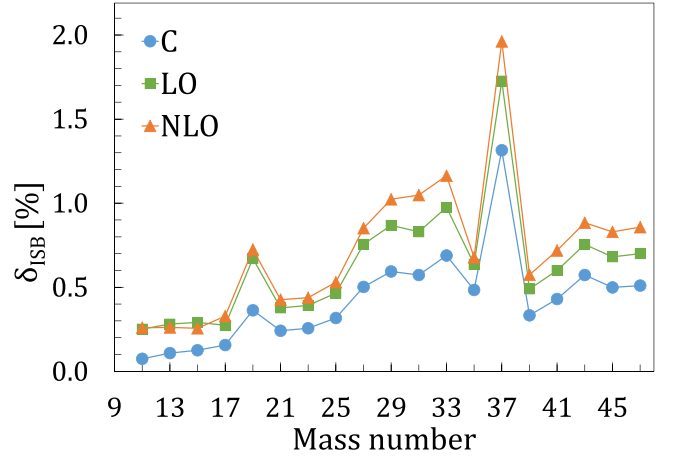
an anomalous case must be treated as an outlier and removed from further analysis of V_{ud}, which was in fact done in Ref. [10]. At the MR-DFT level of approximation there is no cure for such an effect. Hence, the large values of δ_{ISB} for $A = 37$ and, to a lesser extend, for $A = 19$ mirror decays, caused by the same $1s_{1/2} - 0d_{3/2}$ unphysical mixing, should be also rejected from further analysis of V_{ud}. This, in turn, would limit the V_{ud} analysis within the MR-DFT to the two well-measured cases only making the entire procedure statistically questionable.

With the development of DFT-NCCI [11], however, we have at our disposal a new theoretical tool, which allows us to control, at least to some extent, such an unwanted mixing. The model provides rediagonalization of the entire Hamiltonian within the model space that includes the interacting mean-field configurations. We, therefore, decided to analyze all four well-measured $A = 19$, 21, 35, and 37 mirror decays using this formalism. Moreover, in the present work DFT-NCCI calculations were limited to one-particle-one-hole (p − h) configurations only. Such approach was widely tested in our previous β-decay calculation reported in Ref. [32]. The calculated ground-state (gs) and excited p − h configurations in the four mirror nuclei are axially deformed, which implies that the number of participating p − h configurations is very limited due to the K quantum number conservation. In such case, the configuration mixing, which proceeds through spherically symmetric Hamiltonian, is effective only within the collective subspace built upon HF configurations of the same K. In $A = 19$ and $A = 37$ the gs configuration is built upon $K = 1/2$ Nilsson state having the spin $I = 1/2$ and $I = 3/2$, respectively. Hence, the mixing is effective within 3 HF configurations having $\Delta K = 0$. These configurations are built upon one of the three active $K = 1/2$ Nilsson orbits [220 1/2], [200 1/2], and [211 1/2] originating from the $d_{5/2}$, $s_{1/2}$, and $d_{3/2}$ spherical subshells, respectively. In $A = 21$ and $A = 35$ the gs spin is $I = K = 3/2$. The active model space then consists of only two HF configurations built upon either
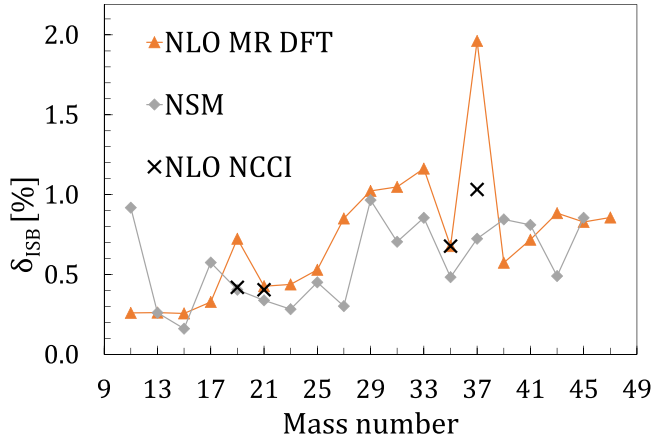
FIG. 3. ISB corrections to the Fermi branch of ground-state β decay in $T = 1/2$ mirror nuclei calculated using NLO (orange triangles) of our MR-DFT model in comparison with the nuclear shell model (NSM) results (gray diamonds) taken from Ref. [3]. Black crosses mark the DFT-NCCI results for $A = 19$, 21, 35, and 37 decays, see Table II.

the [211 3/2] or [202 3/2] Nilsson orbits originating from $d_{5/2}$ and $d_{3/2}$ spherical subshells.

Large energy gap between [211 3/2] or [202 3/2] Nilsson orbits decreases considerably the effect of configuration mixing on $\delta_{\mathrm{ISB}}^{\mathrm{V}}$ in $A = 21$ and $A = 35$. In contrast, the effect is very strong in $A = 19$ and $A = 37$. For the ^{19}Ne $\rightarrow$ ^{19}F, in the NLO variant, the ISB correction $\delta_{\mathrm{ISB}}^{\mathrm{V}}$ drops from 0.738% calculated for the single configuration representing the ground state to 0.580% after admixing the first excited configuration and further to 0.430% after admixing the second excited configuration. For the ^{37}K $\rightarrow$ ^{37}Ar decay the ISB correction decreases from 1.833% to 1.099% and down to 1.042%, respectively. Note that the configuration mixing in $A = 19$ and 37 corrects, to large extent, the irregular behavior of $\delta_{\mathrm{ISB}}^{\mathrm{V}}$ versus A obtained for these two cases in MR-DFT, see Fig. 3. The referential list of our best estimates of $\delta_{\mathrm{ISB}}^{\mathrm{V}}$ values is given in Table I. For $A = 19$, 21, 35, and 37 the value obtained with DFT-NCCI calculations is provided. Otherwise, MR-DFT results are listed.

Table II summarizes the results of DFT-NCCI calculations. It contains the results for the calculated values of $\delta_{\mathrm{ISB}}^{\mathrm{V}}$, the average values of nucleus independent reduced lifetime $\bar{\mathcal{F}}t_0$

TABLE I. ISB corrections $\delta_{\mathrm{ISB}}^{\mathrm{V}}$ to the Fermi transitions in sd-shell nuclei calculated using the NLO variants of MR-DFT and DFT-NCCI model (the latter values are labeled with asterisk).

A	$\delta_{\mathrm{ISB}}^{\mathrm{V}}$	A	$\delta_{\mathrm{ISB}}^{\mathrm{V}}$
17	0.34(3)	29	1.03(10)
19	0.430(56)*	31	1.06(11)
21	0.415(54)*	33	1.17(12)
23	0.45(4)	35	0.688(89)*
25	0.54(5)	37	1.04(14)*
27	0.86(9)	39	0.58(6)

TABLE II. ISB corrections $\delta_{\mathrm{ISB}}^{\mathrm{V}}$ to the Fermi transitions in $A = 19$, 21, 35, and 37 calculated using the NSM [3] and the C, LO, and NLO variants of DFT-NCCI model. Last three rows show the results for $\bar{\mathcal{F}}t_0$, V_{ud}, and for the unitarity test obtained by averaging over the results in $A = 19$, 21, 35 and 37.

	A	NSM	C	LO	NLO
	19	0.415(39)	0.231(30)	0.412(54)	0.430(56)
$\delta_{\mathrm{ISB}}^{\mathrm{V}}$	21	0.348(27)	0.251(33)	0.394(50)	0.415(54)
	35	0.493(46)	0.474(62)	0.647(84)	0.688(89)
	37	0.734(61)	0.714(93)	0.97(13)	1.04(14)
$\bar{\mathcal{F}}t_0$		**6162(15)**	**6166(18)**	**6156(18)**	**6152(21)**
V_{ud}		0.9727(14)	0.9725(14)	0.9732(14)	0.9736(16)
unitarity		0.9967(31)	0.9961(31)	0.9976(31)	0.9983(35)

defined, for a single transition, as:

$$\mathcal{F}t_0 \equiv \mathcal{F}t^{\mathrm{mirror}} \left(1 + \frac{f_A}{f_V} \varrho^2 \right), \qquad (9)$$

the extracted values of V_{ud}, and the result of the unitarity test. Note that the DFT-NCCI theory for V_{ud} is convergent with respect to addition of higher-order ISB terms as depicted in Fig. 4 and that the final V_{ud} matrix element

$$V_{\mathrm{ud}} = 0.9736 \pm 0.0016$$

lies within $\frac{1}{2}\sigma$ from the value assessed from superallowed $0^+ \rightarrow 0^+$ Fermi transitions, which is $V_{\mathrm{ud}} = 0.97417 \pm 0.00021$ [1]. In the calculations of $\bar{\mathcal{F}}t_0$ and V_{ud} we used the radiative corrections and phase-space factors taken from Ref. [3]. The experimental data were taken from Refs. [33,34] in case of $A = 19$ where we have taken an error-weighted sum of a half-life time reported from these independent experiments, the same for $A = 21$ [35,36], $A = 35$ [4], and for $A = 37$ [7].
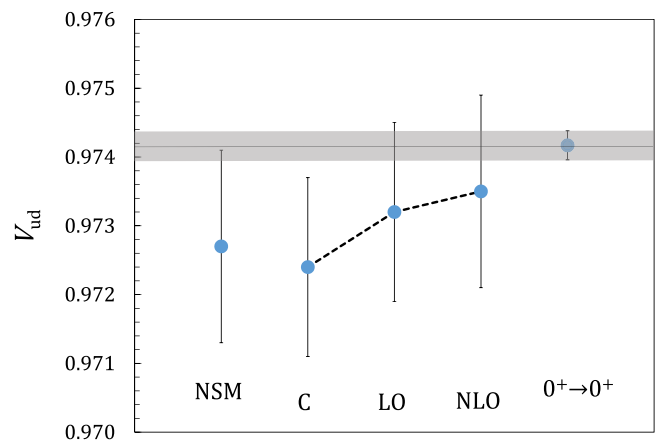

FIG. 4. V_{ud} matrix element calculated from the $T = 1/2$, $A = 19$, 21, 35, and 37 mirror decays by means of the NSM [3] and the three variants C, LO, and NLO of the DFT-NCCI model. Right point represents the V_{ud} obtained from superallowed Fermi β decays taken from Ref. [1].

TABLE III. Configurations used in the DFT-NCCI calculations for $A = 21$ $T = 1/2$ mirrors. Full dots denote pairwise occupied Nilsson states, left (blue) and right (red) side of each column presents different type of nucleons. In the case of ^{21}Na on the left (blue) the table shows neutrons whereas on the right protons (red). Up (down) arrows denote singly occupied Nilsson states with positive (negative) K quantum numbers, respectively. Note that excitation of a pair to the $|202\ 5/2\rangle$ Nilsson level leads to oblate shape.

group	PROLATE									group	OBLATE		
config.	g.s.	ν=1				nn/pp	np	nn/pp	ν=3	config.	g.s.	nn/pp	np
total K	3/2	1/2	1/2	1/2	3/2	3/2	3/2	3/2	3/2	total K	3/2	3/2	3/2
kernel	1	2	3	4	5	6	7	8	9	kernel	10	11	12
$\vert 202\,3/2\rangle$					↑								
$\vert 211\,1/2\rangle$		↑							↑	$\vert 200\,1/2\rangle$			
$\vert 200\,1/2\rangle$			↑					●	↓	$\vert 220\,1/2\rangle$			
$\vert 202\,5/2\rangle$										$\vert 211\,3/2\rangle$	↑	● ↑	↑ ●
$\vert 211\,3/2\rangle$	↑	●				● ↑	↑ ●	↑	↑	$\vert 202\,5/2\rangle$	● ●	●	↓ ↑
$\vert 220\,1/2\rangle$	● ●	● ↑	● ●	● ●	● ●	●	↑ ↓	●	●				

C. Theoretical uncertainty analysis

Let us finally comment on theoretical uncertainties. The overall uncertainty imposed on the calculated ISB comes from three major sources: (i) from the cutoff on harmonic oscillator basis, (ii) from the uncertainties of the class-III LECs, and finally (iii) from the configuration mixing. The uncertainties associated with the first two sources can be reliably estimated and do not exceed ≈5%. The uncertainty associated with configuration mixing can be evaluated only *a posteriori*, after performing configuration-interaction calculations in the larger configuration space.

In order to assess the uncertainty associated with configuration mixing we decided to perform configuration-interaction calculations for two representative cases $A = 21$ and $A = 37$. In the case of ^{21}Na $\rightarrow$ ^{21}Ne decay we increased the model space to 12 axially deformed configurations, which are depicted schematically in Table III. The result of the calculation is shown in Fig. 5. The figure presents a relative change in
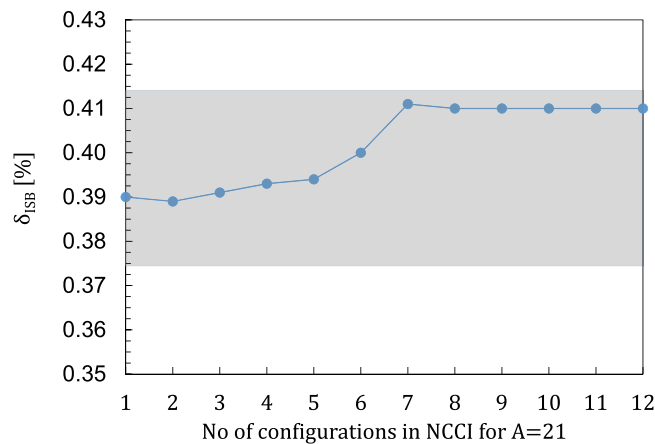

FIG. 5. ISB correction to the Fermi transition ^{21}Na $\rightarrow$ ^{21}Ne with respect to an increase of a configuration space involving $1p - 1h$ and $2p - 2h$ pairing-type excitations. Configurations are added in the order listed in Table III. Shaded area marks 5% error bar superimposed on DFT-NCCI result calculated using $1p - 1h$ configurations. The calculation was performed for LO variant of the isovector interaction, see Eq. (4) using the single-particle basis consisting $N = 12$ harmonic oscillators shells.

the calculated ISB correction with respect to the value quoted in Table II. As shown in the figure, admixture of seniority one $1p - 1h$ excitations (configurations no. 1–5) does not bring any relevant effect on δ_{ISB}. A perceptible increase can be noticed after admixing of nn-, pp-, and np-pairing-type $2p - 2h$ excitations in the configuration space. The amount of the increase is around 5%, which means that for this, and most likely $A = 35$ case, our predictions can be considered as very stable with respect to the configuration mixing.

We performed similar calculation for the irregular and therefore most difficult case of ^{37}K $\rightarrow$ ^{37}Ar transition. In the analysis we included seven configurations depicted in Table IV. The calculation indicates, see Fig. 6, that the total estimated error due to configuration mixing in this case is of the order of 15%. It might be even slightly larger after including more $2p - 2h$ excitations. However, proximity of Nilsson orbitals provoking unstable HF solutions disables performance of such analysis. Nevertheless, at the moment, there is no strong motivation for conducting such a study. Theoretical error associated with the δ_{ISB} calculation constitutes only a tiny fraction in the total error budget of $|V_{\mathrm{ud}}|$, which is completely dominated by experimental uncertainties [4]. In conclusion, we have imposed 15% error on our irregular δ_{ISB}

TABLE IV. Configurations used in the DFT-NCCI calculations for $A = 37$ $T = 1/2$ mirrors. Full dots denote pairwise occupied Nilsson states, left (blue) and right (red) side of each column presents different type of nucleons. In the case of ^{37}K on the left (blue) the table shows neutrons whereas on the right protons (red). Up (down) arrows denote singly occupied Nilsson states with positive (negative) K quantum numbers, respectively.

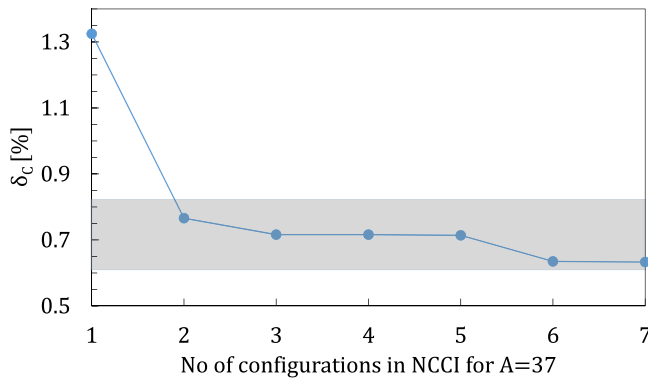| group	OBLATE						
config.	g.s.	ν=1			nn/pp	ν=3	ν=1
total K	1/2	3/2	1/2	1/2	1/2	1/2	3/2
kernel	1	2	3	4	5	6	7
$\vert 211\,1/2\rangle$	↑	●	●	●	● ↑	↓ ↑	●
$\vert 202\,3/2\rangle$	● ●	● ↑	● ●	● ●	● ●	● ●	● ●
$\vert 200\,1/2\rangle$	● ●	● ●	● ↑	● ●	● ●	● ●	● ●
$\vert 220\,1/2\rangle$	● ●	● ●	● ●	● ↑	● ●	● ↑	● ●
$\vert 211\,3/2\rangle$	● ●	● ●	● ●	● ●	● ●	● ●	● ↑
$\vert 202\,5/2\rangle$	● ●	● ●	● ●	● ●	● ●	● ●	● ●

FIG. 6. ISB correction to the Fermi transition ^{37}K $\to$ ^{37}Ar with respect to an increase of a configuration space involving $1p-1h$ and $2p-2h$ pairing-type excitations. Configurations are added in the order listed in Table IV. Shaded area marks 15% error bar superimposed on DFT-NCCI result calculated using $1p-1h$ configurations. The calculation was performed using the single-particle basis consisting $N = 12$ harmonic oscillators shells with the Coulomb as the only source of isospin-symmetry breaking.

in $A = 19$ and $A = 37$ and 5% error in regular $A = 21$ and $A = 35$ cases due to configuration mixing.

Let us finally mention that our results are obviously a subject to systematic error associated with the form and parameters of the employed EDF. Our earlier calculations, see Ref. [12], as well as the random-phase approximation calculations by Liang *et al.* [37] suggest that variations in EDF parametrizations should rather weakly influence the extracted V_{ud}. Detailed analysis of such uncertainties, however, is very difficult and will not be performed here. As already mentioned the total error budget of $|V_{ud}|$ is, at present, dominated by experimental uncertainties [4].

The uncertainty analysis performed above allows us to conjecture that our MR-DFT predictions presented in Fig. 3 can be considered as relatively stable with respect to the configuration mixing. Hence, with the exception of $A = 19$ and $A = 37$ decays where the DFT-NCCI calculations are indispensable, the MR-DFT values of δ_{ISB} can be treated as recommended after superimposing, on average, 10% error due to configuration mixing. At present, due to the accuracy of current experimental data, better accuracy of theoretical corrections is not needed what allows us to refrain in this work from performing time-consuming systematic computations of δ_{ISB} using the DFT-NCCI framework. Such calculations can be always performed upon request. In turn, the conjecture allows us to conclude, see Fig. 3, that our calculations for δ_{ISB} are in overall good agreement with the results of NSM calculations with the exception of the very few cases such as $A = 11$ and $A = 27$, which need to be examined separately.

IV. CONCLUSIONS

In this paper, we performed systematic study of isospin impurities to the nuclear wave functions in $T = 1/2$ mirror nuclei using MR-CDDFT that includes, apart from the Coulomb interaction, the class-III ISB interaction adjusted to reproduce the Nolen-Schiffer anomaly in MDEs. We have

investigated the impurities using three variants of the model including different ISB forces, namely: (i) involving only the Coulomb force, (ii) involving the Coulomb and LO contact ISB forces, and (iii) involving the Coulomb and local ISB forces up to NLO. We have demonstrated, for the first time, that the class-III interaction very strongly increases isospin mixing, see Fig. 1. Our results show that the NLO theory is convergent and brings much smaller increase of α_{ISB} as compared to the LO theory.

Next, we present a profound impact of class-III force on the isospin-symmetry-breaking corrections δ^V_{ISB} to the Fermi matrix elements of ground-state decays of $T = 1/2$ mirror nuclei, which constitute a theoretical input for the precision tests of the electroweak sector of the SM. In order to assess the effect quantitatively we performed systematic study of δ^V_{ISB} using MR-DFT with the three variants of the ISB force described above. As expected from the α_{ISB} study, we observe strong systematic increase in δ^V_{ISB} after including the LO class-III force and further, albeit much smaller, increase within the NLO theory.

The δ^V_{ISB} calculated using MR-DFT show irregularities for $A = 19$ and 37 cases, which are among the decays that are used for the SM test. Such irregularities usually indicate a mixing among the active Nilsson orbitals, which can be taken care of by performing configuration-interaction calculations. In order to verify this conjecture and make our predictions more precise we performed the DFT-NCCI calculations of the ISB corrections in $A = 19$, 21, 35, and 37 $T = 1/2$ mirrors. Since these nuclei are axial we have limited the DFT-NCCI model space to particle-hole deformed Nilsson configurations with $\Delta K = 0$, with respect to K quantum number of the ground-state configuration. The DFT-NCCI results are collected in Table II. The values of δ^V_{ISB} calculated using the LO and NLO theories are systematically larger than the results obtained using only the Coulomb interaction. There are also systematically larger than the corrections calculated using the NSM in Ref. [3]. In turn, the extracted central value of V_{ud} matrix element is closer to the value obtained using data on $0^+ \to 0^+$. Our $|V_{ud}| = 0.9736(16)$ was obtained with the error-weighted average over four mirror ($A = 19$, 21, 35, and 37) transitions excluding the outlier $A = 29$, a case measured with a lesser accuracy as compared to other cases see Ref. [4]. This value is considerably larger than the one, $|V_{ud}| = 0.9727(14)$, given in Ref. [7] and above the value $|V_{ud}| = 0.9730(14)$ of Ref. [38], which includes also the $A = 29$ decay in the average.

The results presented here for δ^V_{ISB} and $|V_{ud}|$ are very consistent with the NSM results. This further increases a confidence that the MR-DFT and DFT-NCCI models are reliable theoretical tools allowing to assess quantitatively diverse isospin-symmetry-breaking phenomena in atomic nuclei from MDEs and TDEs in nuclear binding energies, as shown in Refs. [21,22], through mirror energy displacements (MEDs) versus angular momentum calculated recently in Refs. [39,40] to a very subtle pseudo-observables such as isospin impurities and corrections to Fermi decays as shown here and in Refs. [9,10]. The results of MR-DFT or DFT-NCCI calculations for these isospin-sensitive observables are comparable or, sometimes, only slightly worse as compared to the

results of fine-tuned state-of-the-art NSM communicated in Refs. [2,13,41] and references quoted therein. This, in turn, seems to create new opportunities for comparative studies of the NSM and DFT-rooted models, which can possibly shed new light on the role of different sources of isospin symmetry breaking and resolve certain *ad hoc* assumptions present in both models. Such studies, however, are beyond the scope of this work and are planned to be undertaken in the future.

[1] J. C. Hardy and I. S. Towner, Phys. Rev. C **91**, 025501 (2015).

[2] J. C. Hardy and I. S. Towner, Phys. Rev. C **102**, 045501 (2020).

[3] N. Severijns, M. Tandecki, T. Phalet, and I. S. Towner, Phys. Rev. C **78**, 055501 (2008).

[4] O. Naviliat-Cuncic and N. Severijns, Phys. Rev. Lett. **102**, 142302 (2009).

[5] N. Severijns, M. Beck, and O. Naviliat-Cuncic, Rev. Mod. Phys. **78**, 991 (2006).

[6] P. Gysbers *et al.*, Nature Phys. **15**, 428 (2019).

[7] B. Fenker, A. Gorelov, D. Melconian, J. A. Behr, M. Anholm, D. Ashery, R. S. Behling, I. Cohen, I. Craiciu *et al.*, Phys. Rev. Lett. **120**, 062502 (2018).

[8] J. A. Nolen, Jr. and J. P. Schiffer, Ann. Rev. Nucl. Sci. **19**, 471 (1969).

[9] W. Satuła, J. Dobaczewski, W. Nazarewicz, and M. Rafalski, Phys. Rev. Lett. **103**, 012502 (2009).

[10] W. Satuła, J. Dobaczewski, W. Nazarewicz, and M. Rafalski, Phys. Rev. Lett. **106**, 132502 (2011).

[11] W. Satuła, P. Bączyk, J. Dobaczewski, and M. Konieczka, Phys. Rev. C **94**, 024306 (2016).

[12] W. Satuła, J. Dobaczewski, W. Nazarewicz, and M. Rafalski, Phys. Rev. C **81**, 054310 (2010).

[13] W. E. Ormand and B. A. Brown, Nucl. Phys. A **491**, 1 (1989).

[14] T. Suzuki, H. Sagawa, and N. Van Giai, Phys. Rev. C **47**, R1360(R) (1993).

[15] B. A. Brown, W. A. Richter, and R. Lindsay, Phys. Lett. B **483**, 49 (2000).

[16] A. P. Zuker, S. M. Lenzi, G. Martinez-Pinedo, and A. Poves, Phys. Rev. Lett. **89**, 142502 (2002).

[17] J. Carlson, S. Gandolfi, F. Pederiva, S. C. Pieper, R. Schiavilla, K. E. Schmidt, and R. B. Wiringa, Rev. Mod. Phys. **87**, 1067 (2015).

[18] A. Petrovici, Phys. Rev. C **91**, 014302 (2015).

[19] K. Kaneko, Y. Sun, T. Mizusaki, S. Tazaki, and S. Ghorui, Phys. Lett. B **773**, 521 (2017).

[20] X. Roca-Maza, G. Colò, and H. Sagawa, Phys. Rev. Lett. **120**, 202501 (2018).

[21] P. Bączyk, J. Dobaczewski, M. Konieczka, W. Satuła, T. Nakatsukasa, and K. Sato, Phys. Lett. B **778**, 178 (2018).

[22] P. Bączyk, W. Satuła, J. Dobaczewski, and M. Konieczka, J. Phys. G: Nucl. Part. Phys. **46**, 03LT01 (2019).

[23] E. M. Henley and G. A. Miller, *Mesons in Nuclei*, edited by M. Rho and D. H. Wilkinson (North Holland, Amsterdam, 1979).

[24] G. A. Miller and W. H. T. van Oers, *Symmetries and Fundamental Interactions in Nuclei*, edited by W. C. Haxton and E. M. Henley (World Scientific, Singapore, 1995).

[25] P. Ring and P. Schuck, *The Nuclear Many-Body Problem* (Springer, Berlin, 1980).

[26] D. Varshalovich, A. Moskalev, and V. Khersonskii, *Quantum Theory of Angular Momentum* (World Scientific, Singapore, 1988).

[27] J. Dobaczewski, W. Satuła, B. Carlsson, J. Engel, P. Olbratowski, P. Powałowski, M. Sadziak, J. Sarich, N. Schunck, A. Staszczak, M. Stoitsov, M. Zalewski, and H. Zduńczuk, Comput. Phys. Commun. **180**, 2361 (2009).

[28] N. Schunck, J. Dobaczewski, W. Satuła, P. Bączyk, J. Dudek, Y. Gao, M. Konieczka, K. Sato, Y. Shi, X. Wang, and T. Werner, Comput. Phys. Commun. **216**, 145 (2017).

[29] M. Beiner, H. Flocard, N. Van Giai, and P. Quentin, Nucl. Phys. A **238**, 29 (1975).

[30] M. Konieczka, P. Bączyk, and W. Satuła, Phys. Rev. C **93**, 042501(R) (2016).

[31] E. Chabanat, P. Bonche, P. Haensel, J. Meyer, and R. Schaeffer, Nucl. Phys. A **627**, 710 (1997).

[32] M. Konieczka, M. Kortelainen, and W. Satuła, Phys. Rev. C **97**, 034310 (2018).

[33] S. Triambak, P. Finlay, C. S. Sumithrarachchi, G. Hackman, G. C. Ball, P. E. Garrett *et al.*, Phys. Rev. Lett. **109**, 042301 (2012).

[34] L. J. Broussard, H. O. Back, M. S. Boswell, A. S. Crowell, P. Dendooven, G. S. Giri, C. R. Howell, M. F. Kidd, K. Jungmann *et al.*, Phys. Rev. Lett. **112**, 212301 (2014).

[35] J. Grinyer *et al.*, Phys. Rev. C **91**, 032501(R) (2015).

[36] P. D. Shidling, R. S. Behling, B. Fenker, J. C. Hardy, V. E. Iacob, M. Mehlman, H. I. Park, B. T. Roeder, D. Melconian *et al.*, Phys. Rev. C **98**, 015502 (2018).

[37] H. Liang, N. V. Giai, and J. Meng, Phys. Rev. C **79**, 064316 (2009).

[38] M. Gonzalez-Alonso, O. Naviliat-Cuncic, and N. Severijns, Prog. Part. Nucl. Phys. **104**, 165 (2019).

[39] R. D. O. Llewellyn, M. A. Bentley, R. Wadsworth, J. Dobaczewski, W. Satuła, H. Iwasaki, G. de Angelis, J. Ash, D. Bazin, P. C. Bender, B. Cederwall, B. P. Crider, M. Doncel, R. Elder, B. Elman, A. Gade, M. Grinder, T. Haylett, D. G. Jenkins, I. Y. Lee *et al.*, Phys. Lett. B **811**, 135873 (2020).

[40] P. Bączyk and W. Satuła, Phys. Rev. C **103**, 054320 (2021).

[41] M. A. Bentley, S. M. Lenzi, S. A. Simpson, and C. A. Diget, Phys. Rev. C **92**, 024310 (2015).